Electronic Supplementary Material (ESI) for Nanoscale.

Electronic Supplementary Information

Title: Role of surface ligands in determining the electronic properties of quantum dot solid and their impact in photovoltaic figure of merits

Authors: Prasenjit N. Goswami, Debranjan Mandal and Arup K. Rath*

Address: CSIR-National Chemical Laboratory, Dr. Homi Bhabha Road, Pune, 411008, India

* Email: ak.rath@ncl.res.in

EXPERIMENTAL SECTION

Chemicals: Lead oxide (99.0%), 1-octadecene (90%), Oleic acid (90%), Bis(trimethylsilyl) sulfide (TMS), $CdCl_2$ (99.99%), Oleylamine (70%), tetradecyl phosphonic acid (TDPA 97%), Titanium isopropoxide (97%), 3-mercapto propanoic acid (>99%), Thioglycolic acid, Thiolactic acid, 3-Chloro-1-propanethiol and Octane were purchased from Sigma Aldrich. Methanol, acetone and toluene were purchased from Alfa Aesar. Solvents used in the reaction are all anhydrous.

$CdCl_2$ precursor preparation: In a typical synthesis, $CdCl_2$ (0.60gm, 3.28mmol) was dissolved in 10 mL Oleylamine with tetradecyl phosphonic acid (TDPA,0.066gm,0.24mmol) under vacuum for 16 hrs at 105°c. The product was kept at 80°C under Ar to avoid solidification.

PbS QD Synthesis: Lead oxide (0.45gm, 2mmol), 1.5 mL oleic acid (4.75mmol) and 3mL 1-Octadecene were mixed in three neck RB flask and kept under vacuum at 95°C for 16 hrs. Reaction mixture was then changed from vacuum to Ar atmosphere. 15 mL 1-Octadecene was added into the reaction mixture at 95°C and the temperature was increased to 120°C. 210µL TMS (1mmol) in 10 mL 1-Octadecene was then injected quickly into the reaction bath and the entire solution turned to black immediately, indicating PbS nucleation. The heating source was switched off and the reaction bath was allowed to cool down naturally. When the temperature reached 80°C, 1 mL $CdCl_2$ precursor was injected into the reaction bath under continuous stirring. The reaction bath was allowed cooling down to room temperature (35°C) without removing the heating source. 60 mL anhydrous acetone was then added to the mixture and kept under continues stirring for next 4 minutes and then switched off the rotation and allows QD's to precipitate. PbS QD's were isolated from the solution by centrifuging at 3500 RPM for 5 minutes. The nanocrystals were then purified by dispersion in toluene and reprecipitation with 1:1 acetone and methanol mixer (volume ratio), then again dispersed in toluene. The nanocrystals were further washed with methanol two times and finally, PbS QD's were dispersed in octane for device fabrication.

TiO_2 sol gel precursor preparation: TiO_2 was prepared following our previously reported method with a small change (Ref-39 of the manuscript). In a typical synthesis titanium isopropoxide (2.4 mmol) was added 2.53 mL of 2-propanol and stirred for 30 minutes. 14µL (5M) HCl was then taken in 2.53 ml of 2-propanol and added to the solution slowly under continuous stirring. The whole solution was then left stirring for another 30 minutes to form the transparent TiO_2 precursor.

TiO_2 film deposition: Commercially available Indium tin oxide (ITO) coated glass was etched by HCl and Zinc dust. Later they were sonicated in the soap solution, acetone and isopropanol for 30 minutes each and finally ITO substrates were cleaned in boiling isopropanol for 10 minutes before n-type layer deposition. The TiO_2 precursor was spin coated at 2500 rpm for 60 seconds on top of ITO surface. The films were then annealed at 170°C for 40 minutes.

Photovoltaic device fabrication: PbS CQDs active layers were constructed by the conventional layer-by-layer method. (Ref: 2 in the manuscript) For PbS@MPA devices 5% v/v 3-MPA in methanol solution was used for ligand exchange. For each PbS layer, 30 mg/ml PbS from Octane solution was deposited on the substrate in dynamic condition at 2500 rpm for 40 seconds. Under continuous spinning 6-7 drops of MPA were added followed by rinsing with 8-9 drops of methanol. The same process was repeated up to 12 layers to achieve the desired thickness. For PbS@TGA and PbS@TLA devices, 10% v/v ligand solutions in methanol were used and the ligand exchange process was repeated two times followed by two times washing with methanol for each PbS layer deposition. Finally, MoO_3 (10 nm)/Au (50 nm)/Ag (100 nm) layer was deposited sequentially using thermal evaporation, at a base pressure of 3×10^{-6} mbar.

I-V measurement under AM1.5 sun: I-V characteristics were measured using a Keithley 2634B source-meter under ambient condition. A.M.1.5 solar illumination was generated using class-AAA solar simulator from Peccell technologies (PEC-L01). The source intensity was adjusted to 100 mW/cm^2 using the Thorlab flat band thermal sensor S302C.

Temperature dependent V_{oc} and J_{sc} measurement: Temperature dependent measurements were carried out using liquid nitrogen cooled cryostat equipment (Janis, Model no.VPF-100) controlled by a Lakeshore temperature controller 325 module. Once the system was cool down to 76K it was kept at this temperature for 30 minutes to stabilize. The instrument was warmed up at a rate of 5 K/min and data was taken from 160K to 300K temperature.

Intensity dependent V_{oc} and J_{sc} measurement: Intensity dependent V_{oc} and J_{sc} were measured using a 658 nm laser source provided by a Laser diode control unit (Newport LQA658-30C) controlled by a function generator (Tektronics, AFG 3021C).

Capacitance-V measurement: Cap–V measurements were performed by PSM1735 (N4L) LCR meter. The measurement was carried out at a frequency of 1KHz and a.c. perturbation voltage of 50mV.

Photo-CELIV measurement: The experimental set up consists of a function generator (Tektronics, AFG 3021C), 658 nm Laser diode (Newport LQA658-30C) and Digital oscilloscope (Tektronics, MDO 3104). Function generator was used generate voltage pulses of a suitable ramp. It was also used to trigger the laser to generate light pulses. The time delay between the laser pulse and voltage ramp were controlled by providing suitable delay time between the pulses using the function generator. Solar cells were kept at reverse bias condition for photo-CELIV measurement. Applied voltage ramp and corresponding current evolution were recorded with the help of digital oscilloscope. In order to record the current evolution, external resistance was set to 50 Ω for the entire measurement range.

Transient Photo Voltage (TPV) and Transient Photo Current (TPC) measurement: TPV and TPC measurements were performed using a Laser diode control unit (Newport LQA658-30C) modulated through a function generator (Tektronics, AFG 3021C) to create perturbation light pulses. A solar simulator (Peccell, PEC-L01) was used to generate constant V_{oc} from the solar cells. Light biasing was varied by neutral density filters used to generate different V_{oc} and J_{sc} values. For TPV measurement device under test was connected to the oscilloscope (Tektronics, MDO 3104) through 1 MΩ resistance. Laser pulse intensities were modulated to keep the perturbation voltage below 10 mV. TPC measurements were carried out using the laser pulse alone and the output was measured across 50 Ω resistance.

S1: Attenuated total reflectance ***FT-IR results***

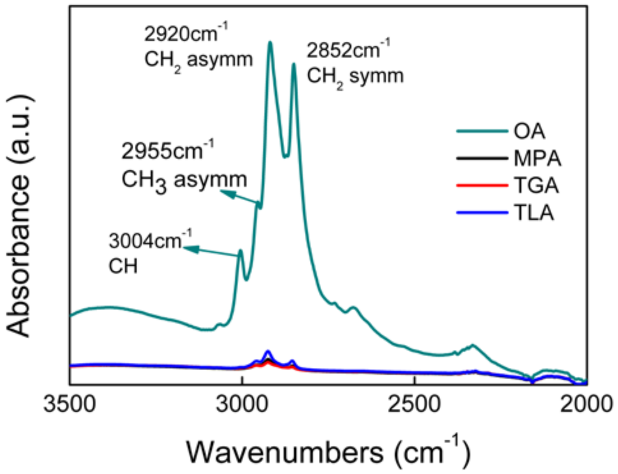

Figure S1. ATR FT-IR spectra under reflective mode for PbS QD films treated with various surface ligands on glass substrate.

Oleic acid capped PbS QD films shows multiple high-intensity peaks within the presented wavenumber (3500-2000 cm-1) range. Peaks correspond to wavenumbers 2955 cm-1 and 3004 cm-1 are assigned as CH3 stretch and CH (-C=C-H) stretch respectively of oleic acid. After ligand exchange with MPA, TGA or TLA both peaks disappeared, suggesting successful ligand exchange process and removal of oleic acid from QD surface. Peaks at 2920 cm-1 and 2652 cm-1 in oleic acid capped PbS QD film correspond to asymmetric and symmetric CH2 stretching frequencies. A substantial decrease in CH2 peak strengths after ligands treatment implies the decrease in CH2 units which suggests successful ligand exchange process. Further, the absence of SH stretching peaks in the range of 2550-2600 cm-1 suggests that sulfur atoms are bonded to the QD surface.

S2: Device stability

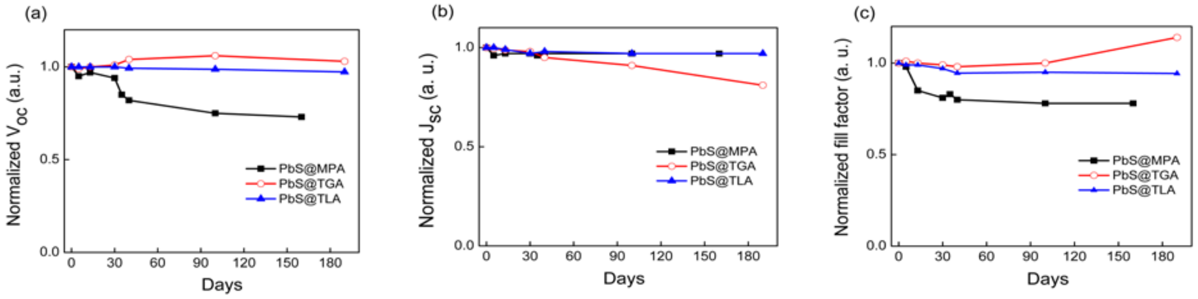

Figure S2. Stability taste of solar cells for different ligand passivation. Evolution of (a) V_{oc}, (b) J_{sc} and (c) fill factor (FF) with time is shown. V_{oc}, J_{sc} and FF values are normalized for clear presentation.

S3: Details of hole mobility and dielectric constant calculation from photo-CELIV measurement:

Hole mobility (μ_h) was determined from the photo-CELIV measurements following equation (ref: 43, 44 of the manuscript)

$$\mu_h = \frac{2d^2}{3At_{max}^2\left(1+0.36\frac{\Delta J}{J_d}\right)} \quad \text{if} \quad \Delta J \le J_d \text{------ (S1)}$$

Where 'd' is device thickness, 'A' is ramp rate, 't_{max}' is the time for the transient current signal to reach its maximum value, 'ΔJ' is the maximum drift current, and 'J_d' is the displacement current.

Relative dielectric constant (ε_m) is determined from the following equation.

$$\varepsilon_m = \frac{J_d d}{A\varepsilon_0} \text{ -----------------------------------(S2)}$$

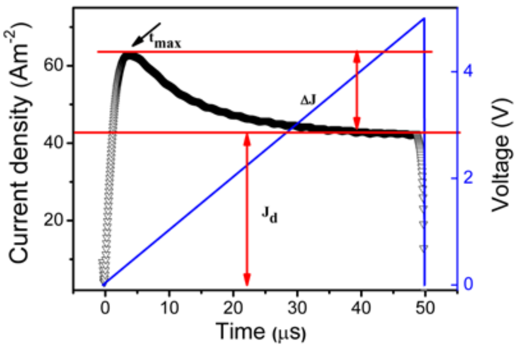

Figure S3. Typical results for CELIV measurements are shown to explain different parameters of equation 1 and 2.

S4: J-V characteristics under dark condition

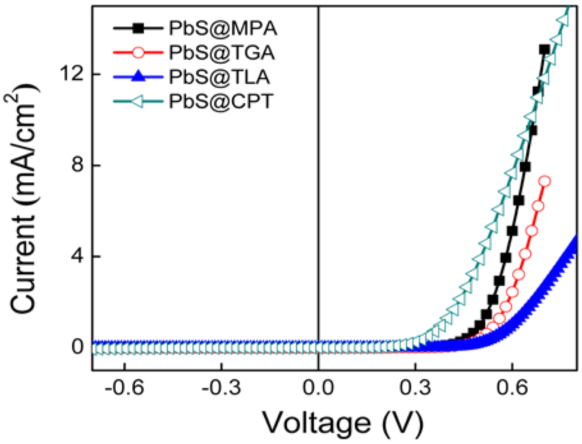

Figure S4. Current density vs voltage plots of solar cells for various surface ligands under dark condition are shown. Series resistances for the respective devices are determined from the slope of J-V characteristics and shown in table S1.

S5: Depletion width and doping density determination from capacitance voltage measurements

Capacitance of a n-p heterojunction solar cell can be written as

$$C = \frac{\varepsilon_0 \varepsilon_r A}{W_d} \quad \text{-- (S3)}$$

Where 'C' is the junction capacitance, 'ε_0' permittivity of air, 'ε_r'relative dielectric constant of PbS layer (determined from photo-CELIV measurement), 'A' area of the device and 'W_d' is depletion width inside PbS.

The activated doping density of different ligand exchanged PbS active layer was determined from the $\frac{1}{C^2}$ vs. V plot using the following equation.

$$N_a = \frac{2}{A^2 q \varepsilon_m \varepsilon_0 \frac{dC^{-2}}{dV}} \text{ ; considering } N_a \ll N_d \text{--- (S4)}$$

Where 'N_a' is the acceptor density of PbS layer, 'N_d' is the donor density of TiO_2 layer; and 'q'is electronic charge.

S6: Recombination limited lifetime (τ), diffusion length (l_{diff}) and drift length (l_{drift}) determination

Recombination limited lifetime is determined from the transient photo voltage (TPV) measurement using the following equation

$\tau = -\frac{kT}{q}\frac{F_1}{\frac{dV_{oc}}{dt}}$ --- (S5)

Where 'τ' is photo carrier life time, 'k' is Boltzmann constant, 'T' is temperature, 'q' is electronic charge, 'F_1' ranges between 1 at low injection and 2 at high injection. In this calculation, we used 'F_1' value 1 and T = 293 K. We have measured $\frac{dV_{oc}}{dt}$ from the linier initial slope of the voltage decay curve. A typical case of voltage decay is shown in figure S6

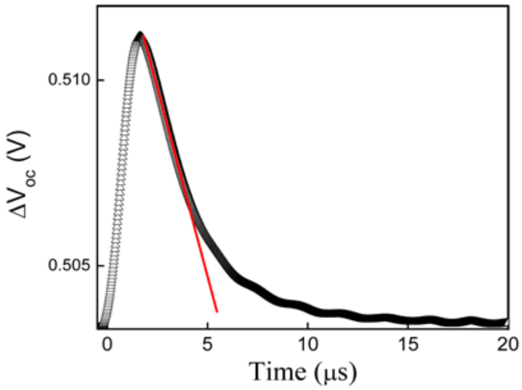

Figure S6. A typical TPV plot showing decay of opencircuit voltage due to application of a small perturbation light pulse.

Carrier diffusion length (l_{diff}) under short-circuit condition is determined as

$l_{diff} = \sqrt{\mu\tau kT/q}$ --- (S6)

where 'μ' is the hole mobility. We have calculated it at 0.9 sun illumination intensity.

The drift length (l_{drift}) is calculated by approximating the linearly varying electric field in depletion region by its average value.

$l_{drift} = \mu\tau V_{bi}/W$ --- (S7)

Where 'V_{bi}' is the built-in potential [$V_{bi}$is determined from the voltage at which J =(J_{light}-J_{dark})=0] and 'W' is the depletion at 0 volt.

S7: Determination of diode ideality factor

Open circuit voltage of a solar cell depend with the light intensity through the following equation

$$V_{oc} = -\frac{p\eta KT}{q}\ln \emptyset + c \text{--} \quad (S8)$$

Where $\emptyset$ is the light intensity, p is the power dependence of short circuit current density with light intensity ($J_{sc} \infty \varphi^{p}$), ‘η’ is the diode ideality factor, ‘K’ is Boltzmann constant, ‘T’ is temperature, ‘q’ is electronic charge and ‘c’ is the fitting parameter. From the slope of V_{oc} vs. ln ϕ we determined the value of η at T=293K.

S8: Absorption spectrum of PbS QD films for different surface ligands

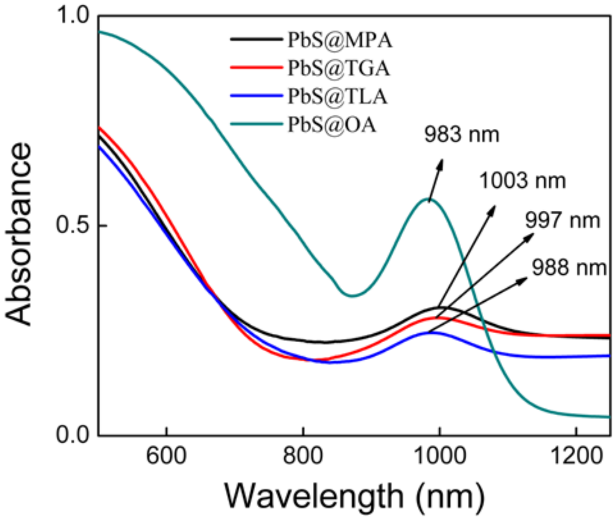

Figure S8. Absorption spectrums of PbS QD films treated with various surface ligands. As compared to oleic acid (OA) capped PbS QDs (measured in Toluene), small red shifts in first excitonic peak position is observed in thin films of MPA, TGA and TLA ligands.

S9: UPS spectra and energy band position of PbS QD films treated with different ligands

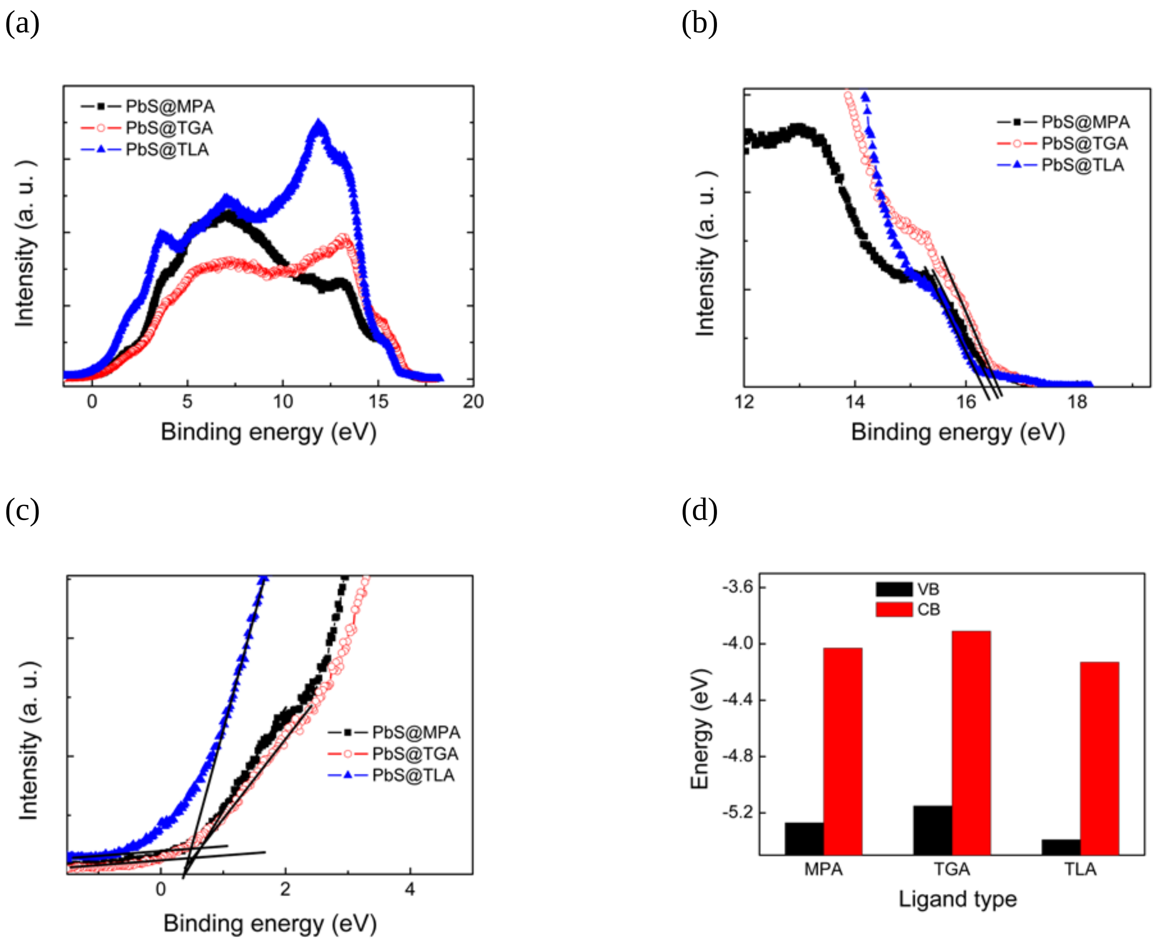

Figure S9. (a) shows the full energy range UPS spectra of PbS QD films for different ligands. (b) and (c) show the magnified view of secondary energy cutoff (SEC) and onset energy region respectively. He-Iα radiation of energy 21.22 eV is used for the UPS measurement. (d) shows the valence band (VB) and conduction band (CB) positions as determined from absorption spectrum and UPS measurement.

Table S1: Series resistance of solar cells treated with different ligand are shown under dark and under solar illumination.

Ligand type	**Series resistance under dark (Ωcm^{-2})**	**Series resistance under solar illumination (Ωcm^{-2})**
PbS@MPA	12.06	7.12
PbS@TGA	18.76	11.84
PbS@TLA	57.64	17.10
PbS@CPT	24.64	16.12

***Table S2**: XPS data analysis of S 2p spectra of PbS QD films treated with different ligands*

Ligand type	Species	Binding energy (eV)	Atomic %
PbS@MPA	Pb-S	160.3	63.3
	S-C	161.38	14.3
	S-S	162.56	12.4
	$PbSO_3$	164.8	6
	$PbSO_4$	166.1	3.9
PbS@TGA	Pb-S	160.3	54.7
	S-C	161.38	20.4
	S-S	162.56	16.1
	$PbSO_3$	164.8	6.4
	$PbSO_4$	166.1	2.2
PbS@TLA	Pb-S	160.3	54.3
	S-C	161.38	20.3
	S-S	162.56	17.5
	$PbSO_3$	164.8	3.9
	$PbSO_4$	166.1	3.9